Fully Monolithically Integrated Wide-Band RF-Source

A. Megej, K. Beilenhoff*, C. Sydlo, and H. L. Hartnagel

Institut für Hochfrequenztechnik, Technische Universität Darmstadt
Merckstr. 25, D-64283 Darmstadt, Germany.
Tel.: +49 6151 16 3262; Fax: +49 6151 16 4367; E-mail: *megej@ieee.org*

∗Now with United Monolithic Semiconductors (UMS),
Route Departementale 128 - BP 46, 91401 Orsay Cedex, France.
E-mail: *Klaus.Beilenhoff@ums-gaas.com*

Abstract

A highly integrated wide-band MMIC RF-source using the heterodyne frequency conversion scheme is presented in this paper. Two oscillators, a mixer, and three corresponding buffer amplifiers find place on a MMIC chip with dimensions of $3.0 \times 1.8\,\text{mm}^2$ manufactured using a commercially available 0.25 µm pHEMT process. The circuit provides RF power within a wide range of f = 3.5 – 6.5 GHz.

I. Introduction

MANY applications, in particular the sensor ones, require signal sources with a very wide tuneable bandwidth of oscillations. Further, one-chip systems are desirable due to the reduced assembly efforts and cost [1]. In particular, high performance HEMT voltage-controlled oscillators are essential if they have to be integrated together with mixers, amplifiers etc. to form a system-on-a-chip. Several successful techniques have been reported in the literature which achieve significant VCO tuning ranges [2–4] using direct VCO tuning.

This paper presents a fully monolithically integrated realization of a signal source that provides RF-power within a wide range of $f = 3.5 - 6.5\,\text{GHz}$, which corresponds to an almost octave bandwidth. The output power of the MMIC is $P_{out} = 8.7 - 14.1\,\text{dBm}$. The highly integrated realization is the first-pass success. It requires a chip area of only $3.0 \times 1.8\,\text{mm}^2$. A commercially available pHEMT process was used to fabricate the circuitry.

II. Design Approach

When considering a fully monolithically integrated VCO design, the bandwidth of oscillations is mainly determined by the capacitance-change ratio of the integrated diodes used. The modern pHEMT processes offer integrated diodes with $C_{max}/C_{min} \approx 3 - 5$ that limit the performance of directly tuned oscillators.

The present design approach makes use of the heterodyne frequency conversion scheme. The block diagram of this approach is shown in Fig. 3. A similar realization was reported in [5] where a source was built using hybrid technique with five MMICs and off-chip VCO tuning.

Here, the core of the RF-source is the fully integrated VCO that oscillates within the range of $f_{VCO} = 22.3 - 26\,\text{GHz}$. The VCO output-signal level is then increased by the corresponding buffer amplifier that is also employed to reduce the influence of the further circuitry to the VCO. The local oscillator and its buffer amplifier is employed to provide the LO signal at an appropriate power level. These signals are then given to the mixer that down-converts the VCO frequency to the desired IF band. Finally, the output signal is increased by the broadband amplifier that is designed using resistive feedback.

As a result, an RF-signal within the band of $3.5 - 6.5\,\text{GHz}$ is achieved from a MMIC whose microphotograph is shown in Fig. 4.

A. VCO Circuit

The voltage-controlled oscillator was designed to provide as wide bandwidth of oscillations as possible. The reflection-type circuit topology was utilized for this reason. Figure 1 demonstrates the principle schematic of the voltage-controlled oscillator together with the buffer amplifier. Design techniques used to increase the bandwidth of oscillations are similar to those presented in [6]. A 1×75 µm pHEMT is employed as the active element. Capacitor C_{FB} induces a negative differential resistance at the input of the oscillating transistor $T_{OSC.}$

Six 10×15 µm planar pHEMT diodes are used for frequency tuning. The series-parallel connection of the tuning diodes helps to reduce the RF-voltage value over each single diode, thus, increasing the effective capacitance-modulation ratio of the configuration. The resonator circuit is completed by the grounded transmission line $TL_{RES.}$

The corresponding buffer amplifier was designed with the aim to reduce the influence of the local oscillator on the VCO behavior. A 4×30 µm pHEMT is used to do this. Another transistor T_{Bias} with the same dimensions is used as a current source to provide DC biasing. The elements $TL_{ST,}$ $L_{ST,}$ and R_{ST} help to active the unconditional stability of the amplifying pHEMT. Two L-networks consisting of $L_{out1,2}$ and $C_{out1,2}$ provide matching between the amplifier output and the input of the mixer.

Fig. 5 shows the measured performance of the buffered VCO that was also manufactured separately for characterization reasons. The circuit provides oscillations within the frequency range of $f_{VCO} = 22.3 - 26.0\,\text{GHz}$. The dependence of the oscillation frequency on the tuning voltage exhibits a non-linear behavior that is typical for this kind of VCO's. The measured output power demonstrates a fairly low variation with tuning voltage and amounts to the value of $P_{out,VCO} = 4.7 \pm 0.7\,\text{dBm}$. The buffered VCO occupies chip area of approximately $1.7 \times 1.0\,\text{mm}^2$. It can be seen in the lower left part of the MMIC in Fig. 4.

B. Local Oscillator

The local oscillator schematic bases on the same design topology as the VCO described above. Also here, a 1×75 µm pHEMT is used as the oscillating transistor. The main difference was the design of the resonator circuit: a grounded transmission line is employed to satisfy the oscillation conditions. The buffered oscillator provides RF-power at $f_{LO} = 19.4\,\text{GHz}$ with output power of $P_{out,LO} = 8\,\text{dBm}$. The corresponding buffer amplifier is designed using the same techniques as in the case of the voltage-controlled implementation. The buffered LO circuit can be found in the upper left part of the chip in Fig. 4.

C. Mixer Circuit

Apart from the voltage-controlled oscillator—if even its configuration is very simple—the most challenging task during this work was to design a mixer circuit that operates within a wide frequency range. The main goal was to reduce the chip-size demand and to achieve conversion gain. The latter condition is especially problematic since the difference in power levels between the VCO and LO signals is not significant (4 vs. 8 dBm).

Because of the above requirements, active mixer topology was chosen. The microwave mixer implemented here bases on a simple single-gate configuration. The schematic of the designed mixer circuit is presented in Fig. 6. A self-biased $4 \times 60\,\mu\text{m}$ pHEMT is employed as the frequency converter. The gate of the active transistor is virtually biased negatively using the resistor R_{FB} in its source path. The separation of different signal frequencies is achieved by employing appropriate matching and filter networks at the mixer output and input. The mixer circuit is located in the upper center part of the MMIC (Fig. 4).

This sub-circuit was not manufactured separately. Therefore, only calculated results can be shown here whereas measured performances of the VCO and LO circuits were considered for these simulations. LO-to-RF isolation was calculated to be better than 10 dB at RF frequencies and better than 20 dB at the LO frequency. The LO-IF and RF-IF isolations both were determined to be better than 30 dB. Figure 7 shows the calculated conversion gain for measured values of $P_{out,VCO}$ and $P_{out,LO}$. This parameter is as high as $G_C = 0.7 \div -4$ dB with decreasing values for lower frequencies. Although the initial simulation had predicted a conversion gain around +1 dB, the increase of losses can be explained by the fact that the actual LO-power level is lower than expected. The performed simulations were confirmed by the measurements of the RF-source performance.

D. Broadband Buffer Amplifier

The buffer amplifier, which increases the power level of the mixer output signal, has to operate in a wide frequency range. Its schematic is shown in Fig. 2. Two 8×75 µm transistors as the active element and current source, respectively. An RLC feedback circuit was used to increase the bandwidth of operation and to achieve the unconditional stability. Two stage LC circuits provide matching at the input and the output. The measured small-signal gain amounts to the value of 10.5 ± 1 dB over the entire band of interest and the output matching is better than -10 dB.

III. Measured RF-Source Performance

As already mentioned above, the circuit was realized using the PH25 pHEMT-process of UMS. The gate-length featured by this process is 0.25 µm.

On-wafer measurements of the RF-source realized were performed using the spectrum analyzer HP8565E. Beforehand, cable losses were determined. Measured frequency and power of the output signal are depicted in Fig. 8. The MMIC provides RF signal within a wide frequency range of $f_{IF} = 3.48 - 6.56\,\text{GHz}$ covering almost an octave. The output power levels are within the range of $P_{out,IF} = 8.7 - 14.1$ dBm with a rapid decrease towards the lower frequency. It is mainly due to lower mixer conversion gain (Fig. 7). This is also the reason why the entire tuneable bandwidth of VCO (down to $f_{VCO} = 22.3$ GHz) could not be used.

Due to the incorporation of the frequency conversion scheme, the output contains some spurious signals. These signal levels were measured to be as high as -22 dBc at $f_{IF} = 3.5$ GHz while gradually reducing to -31 dBc at $f_{IF} = 6.5$ GHz.

The presented RF-source realization is the first-pass success. Therefore, the performance shown can still be improved by performing a re-design of the circuit. So, for example, the tuning range could be increased down to $V_{TUNE} = 0\,\text{V}$ that would further increase the tuneable bandwidth of oscillations.

IV. Conclusion

An MMIC is demonstrated here that provides RF power within a wide frequency range of almost an octave. This realization incorporates frequency conversion scheme and employs two oscillators, a mixer, and three amplifiers that all find place on a single MMIC chip. The RF-source is manufactured using a commercial pHEMT process and does not

require any additional elements. This demonstrates the possibility to realize wide-band RF-source on one single MMICs. The fully monolithically integrated realization presented here significantly reduces assembly efforts and, hence, cost.

ACKNOWLEDGMENT

This work was supported by the ADAM OPEL AG, Rüsselsheim/Germany.

REFERENCES

[1] H. Daembkes, R. Quentin, M. Camiade, K. Beilenhoff, B. Adelseck, O. Schickl, J. Schroth, M. Lajugie, and M. Turin, "Influence of advanced GaAs MMICs on structure and cost of high frequency TR-modules for communication and radar systems for volume markets," in *30th European Microwave Conf. Proc.*, Paris, France, Oct. 2000, vol. 1, pp. 270–273.

[2] J. E. Andrews, T. J. Holden, K. W. Lee, and A. F. Podell, "2.5–6.0 GHz broadband GaAs MMIC VCO," in *IEEE MTT-S Int. Microwave Symp. Dig.*, New York, NY, May 1988, vol. 1, pp. 491–494.

[3] B. N. Scott and G. E. Brehm, "Monolithic voltage controlled oscillator for X and Ku-bands," in *IEEE MTT-S Int. Microwave Symp. Dig.*, Dallas, TX, June 1982, vol. 1, pp. 482–485.

[4] A. Megej, K. Beilenhoff, and H. L. Hartnagel, "Conditions for broadband MMIC voltage-controlled oscillators based on theory and experiments," in *IEEE MTT-S Int. Microwave Symp. Dig.*, Phoenix, AZ, May 2001, vol. 3, pp. 1419–1422.

[5] G. Dietz, S. Moghe, H. Fudem, R. Haubenstricker, and R. Becker, "A 5.9–16.3 GHz agile tuning source using wideband millimeter wave MMIC circuits," in *IEEE Microwave and Millimeter-Wave Monolithic Circuits Symp. Dig.*, Albuquerque, NM, June 1992, vol. 1, pp. 61–64.

[6] A. Megej, K. Beilenhoff, and H. L. Hartnagel, "Fully integrated PHEMT voltage controlled oscillator with very high tuning bandwidth," in *30th European Microwave Conf. Proc.*, Paris, France, Oct. 2000, vol. 1, pp. 176–179.

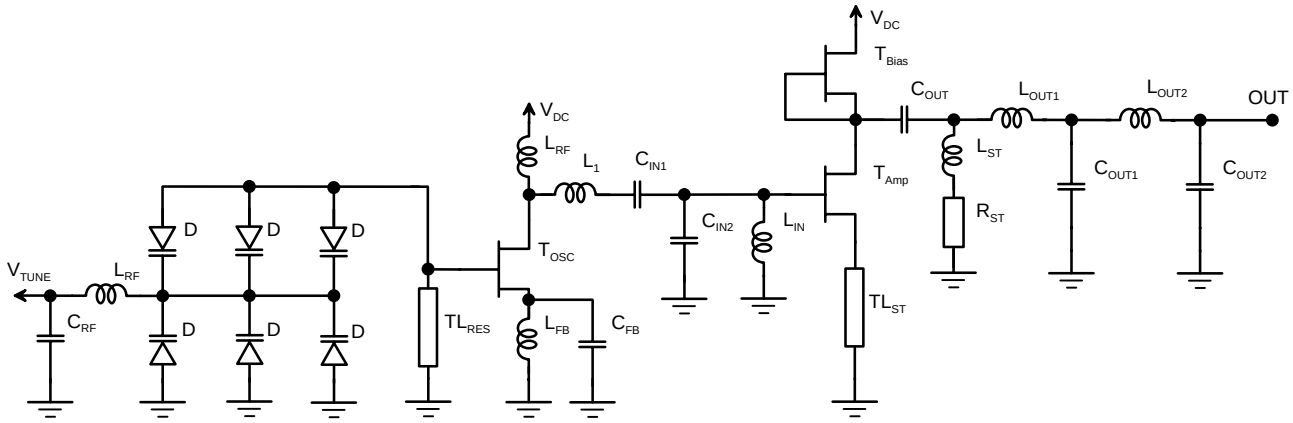

Fig. 1. Principle schematic of the buffered VCO.

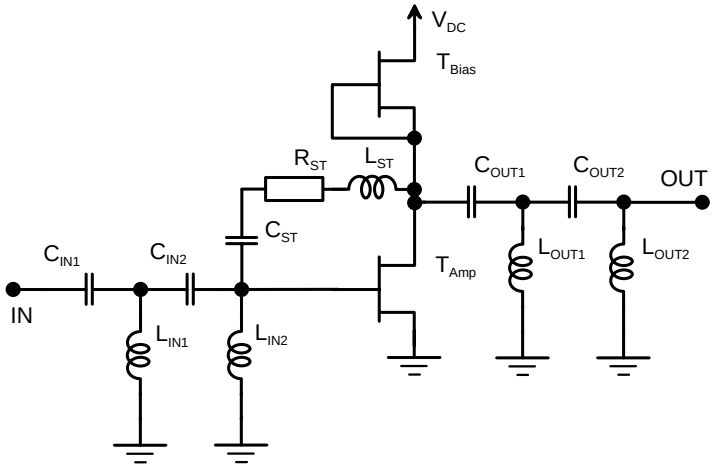

Fig. 2. Schematic of the broadband buffer amplifier.

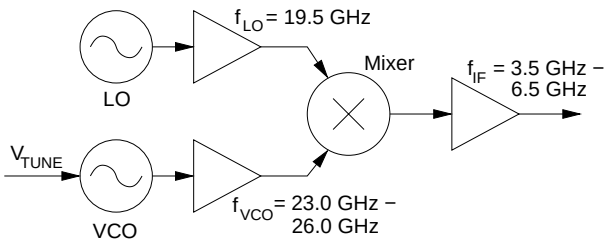

Fig. 3. General schematic of the RF-source considered.

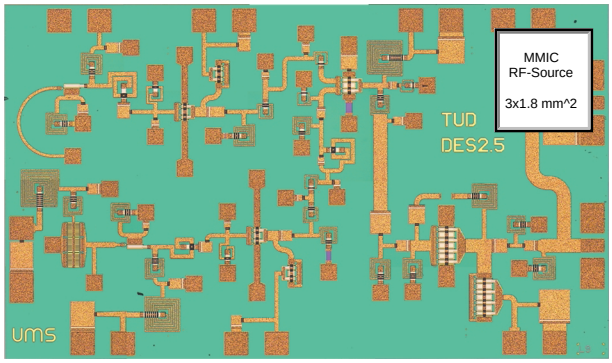

Fig. 4. Microphotograph of the RF-source realized.

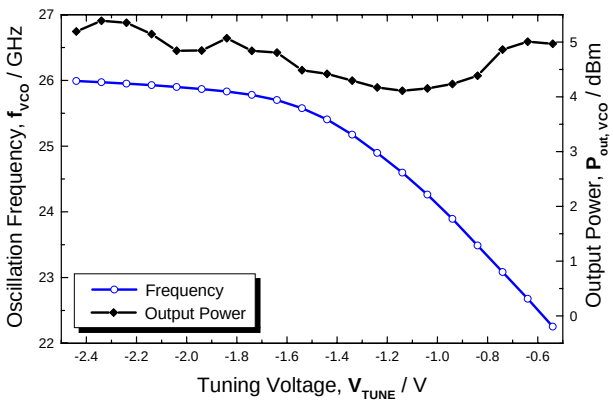

Fig. 5. Measured frequency and output power of the buffered VCO.

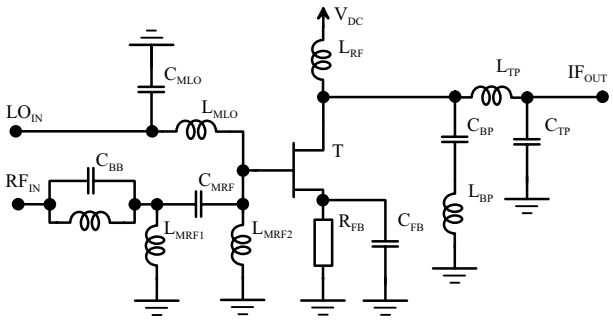

Fig. 6. Principle schematic of the mixer circuit.

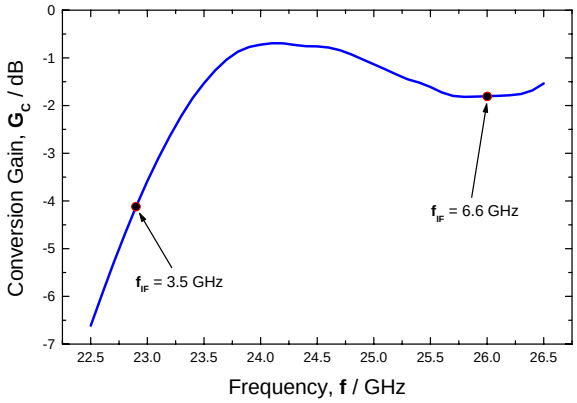

Fig. 7. Mixer conversion gain calculated for measured values of $P_{out,VCO}$ and $P_{out,LO}$.

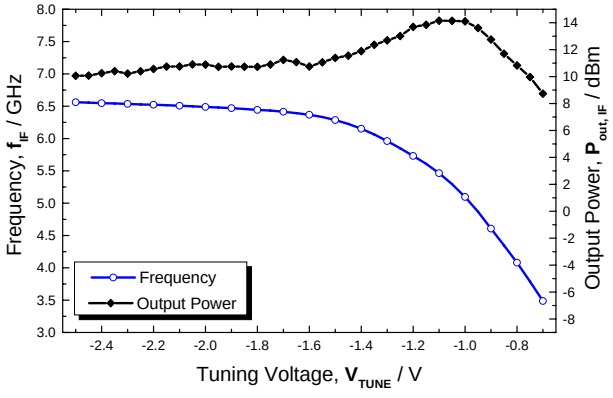

Fig. 8. Measured performance of the RF-Source realized.